Supporting Information for "Femtosecond Charge and Molecular Dynamics of I-containing organic molecules Induced by Intense X-Ray Free-Electron Laser Pulses"

Authors

K. Nagaya[1,2], K. Motomura[3], E. Kukk[3,4], Y. Takahashi[5], K. Yamazaki[5,6], S. Ohmura[1,7], H. Fukuzawa[2,3], S. Wada[2,8], S. Mondal[3], T. Tachibana[3], Y. Ito[3], R. Koga[8], T. Sakai[1], K. Matsunami[1], K. Nakamura[5], M. Kanno[5], A. Rudenko[9], C. Nicolas[10], X.-J. Liu[10,11], C. Miron[10,17], Y. Zhang[12], Y. Jiang[12], J. Chen[13], M. Anand[14,15], D. E. Kim[14,15], K. Tono[16], M. Yabashi[2,16], M. Yao[1], H. Kono[5] and K. Ueda*[2,3]

[1] *Department of Physics, Graduate School of Science, Kyoto University, Kyoto 606-8502, Japan*

[2] *RIKEN SPring-8 Center, Sayo, Hyogo 679-5148, Japan*

[3] *Institute of Multidisciplinary Research for Advanced Materials, Tohoku University, Sendai 980-8577, Japan*

[4] *Department of Physics and Astronomy, University of Turku, FI-20014, Finland*

[5] *Department of Chemistry, Graduate School of Science, Tohoku University, Sendai 980-8578, Japan*

[6] *Department of Chemistry, Graduate School of Science, Hokkaido University, Sapporo 060-0810, Japan*

[7] *Research Center for Condensed Matter Physics, Hiroshima Institute of Technology, Hiroshima 731-5193, Japan*

[8] *Department of Physical Science, Hiroshima University, Higashi-Hiroshima 739-8526, Japan*

[9] *J.R. Macdonald Laboratory, Department of Physics, Kansas State University, 66506 Manhattan, KS, USA*

[10] *Synchrotron SOLEIL, L'Orme des Merisiers, Saint-Aubin, BP 48, FR-91192 Gif-sur-Yvette Cedex, France*

[11] *School of Physics and Nuclear Energy Engineering, Beihang University, Beijing 100191, China*

[12] *Shanghai Advanced Research Institute, Chinese Academy of Sciences, 201210 Shanghai, China*

[13] *Shanghai Institute of Applied Physics, Chinese Academy of Sciences, 201800 Shanghai, China*

[14] *Department of Physics, Center for Attosecond Science and Technology, Pohang University of Science and Technology, Pohang, 37673, South Korea*

[15] *Max Planck Center for Attosecond Science, Max Planck POSTECH/KOREA Res. Init., Pohang, 37673, South Korea*

[16] *Japan Synchrotron Radiation Research Institute (JASRI), Sayo, Hyogo 679-5198, Japan*

[17] *Extreme Light Infrastructure - Nuclear Physics (ELI-NP), "Horia Hulubei" National Institute for Physics and Nuclear Engineering, 30 Reactorului Street, RO-077125 Măgurele, Jud. Ilfov, Romania*

Online supporting information

Our CCE-CE simulation succeeded to reproduce the experimental observations of coincidence measurements when we adopted the parameter set of $T = 300$ K, $\tau = 10$ fs and $R = 0.5$ fs^{-1}. Figures S1 – S4 displays the comparison between the experimental data and CCE-CE model sumulations for I^{q+} coincience data with q=1-4. In each figure, (a)-(e), (f)-(i) and (k)-(n) show the kinetic energy distribution (KED) of fragment ions detected in coincidence with I^{q+}, $SP_2(I^{q+},X)$ and $SP_3(I^{q+},H^+, X)$, respectively, where X represents H^+, O^+, N^+ and C^+. Black lines and red lines correspond to the experimental data and results of CCE-CE simulations. (o) represents the definition of ϕ for $SP_3(I^{q+},H^+, X)$.

In the present SCC-DFTB approach, two types of energy injection to atoms $\{i\}$ were examined. One is the case where the vertical components of additional momenta $\Delta \vec{p}_i$ to the molecular plane, $\Delta \vec{p}_{i\perp}$, are all set to be zero and the other is the case where nonzero momenta are allowed for $\Delta \vec{p}_{i\perp}$. To compare the $\Delta \vec{p}_{i\perp} = 0$ and $\Delta \vec{p}_{i\perp} \neq 0$ cases, we plotted their KED in Fig. S5 and $SP_2(I^{q+}, X)$ in Fig. S6.

Figure S7 shows the spatial distribution of one-electron wave functions for HOMO, HOMO-n (n=1-4) of 5-IU in the ground state, where the atomic position is that we adopted for NAQMD calculations at t=0 fs. Red and green colors represent the isosurfaces of the wave functions with the values of -0.03 and 0.03 atomic units, respectively. It is seen that wave functions of HOMO, HOMO-1 and HOMO-4 are mainly distributed on iodine.

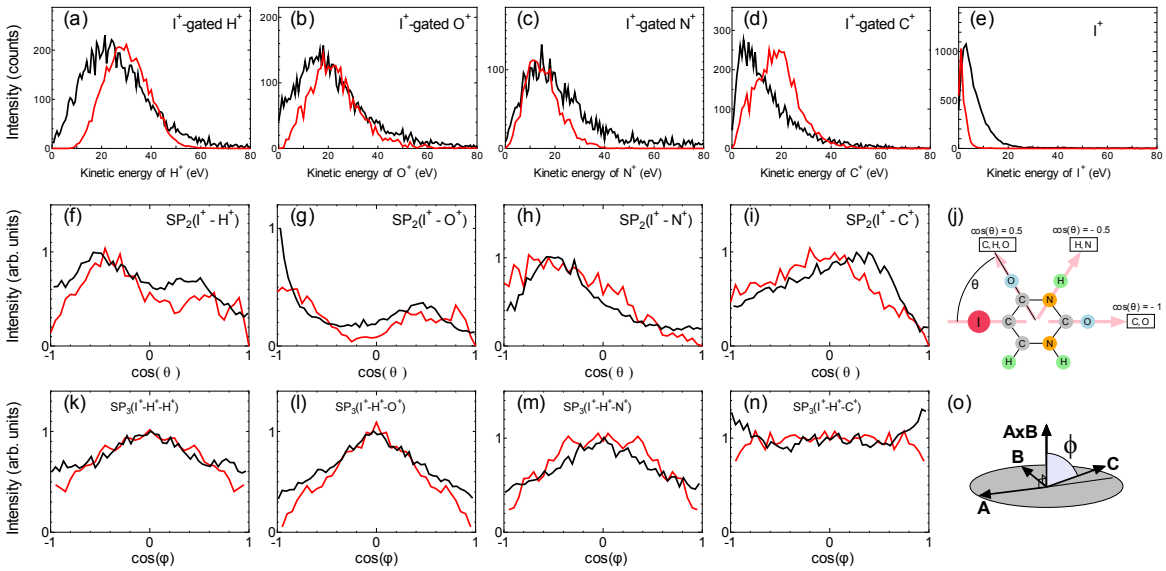

Fig. S1. Comparison between the experiment (black line) and CCE-CE model sumulations (red lines) for I^+ coincience data. (a)-(e) : Kinetic energy distribution of fragment ions. (f)-(i): $SP_2(I^+,X)$ for X=H^+, O^+, N^+ and C^+. (j): Schematics of molecular structure. (k)-(n): $SP_3(I^+,H^+, X)$ for X=H^+, O^+, N^+ and C^+. (o) Definition of ϕ.

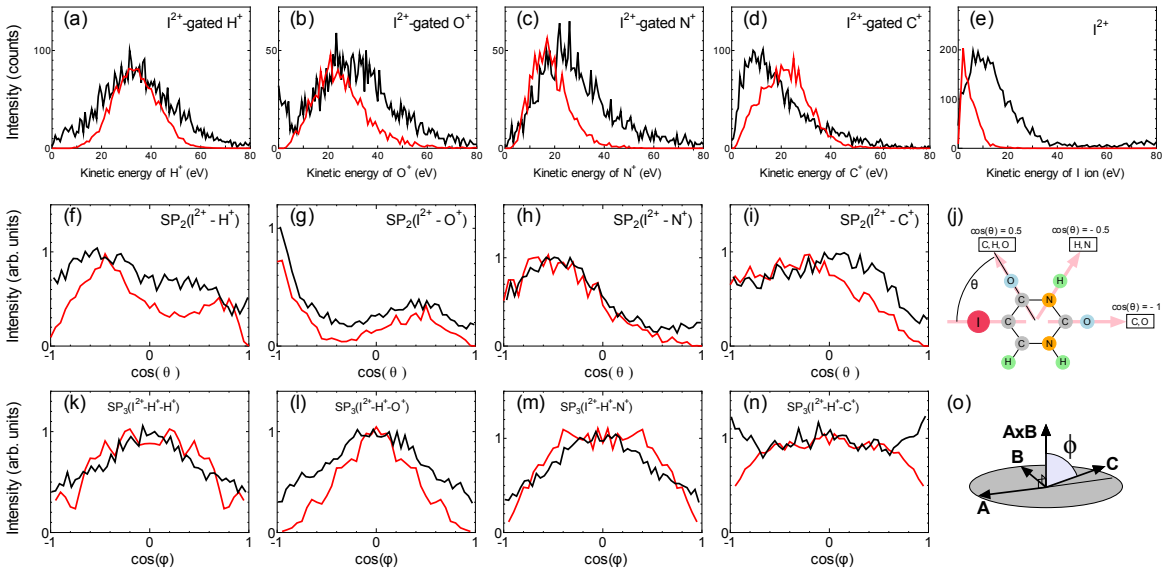

Fig S2. Comparison between the experiment (black line) andCCE-CE model sumulations (red lines) for I^{2+} coincience data. (a)-(e) : Kinetic energy distribution of fragment ions. (f)-(i): $SP_2(I^{2+},X)$ for X=H^+, O^+, N^+ and C^+. (j): Schematics of molecular structure. (k)-(n): $SP_3(I^{2+},H^+, X)$ for X=H^+, O^+, N^+ and C^+. (o) Definition of ϕ.

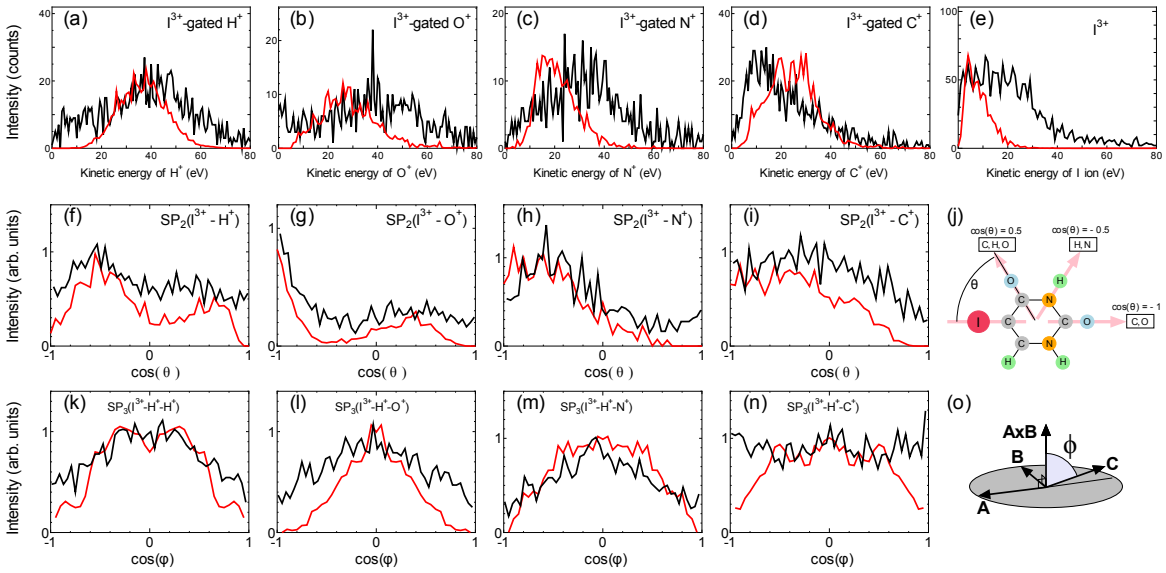

Fig. S3. Comparison between the experiment (black line) and CCE-CE model sumulations (red lines) for I^{3+} coincience data. (a)-(e) : Kinetic energy distribution of fragment ions. (f)-(i): $SP_2(I^{3+},X)$ for X=H^+, O^+, N^+ and C^+. (j): Schematics of molecular structure. (k)-(n): $SP_3(I^{3+},H^+, X)$ for X=H^+, O^+, N^+ and C^+. (o) Definition of ϕ.

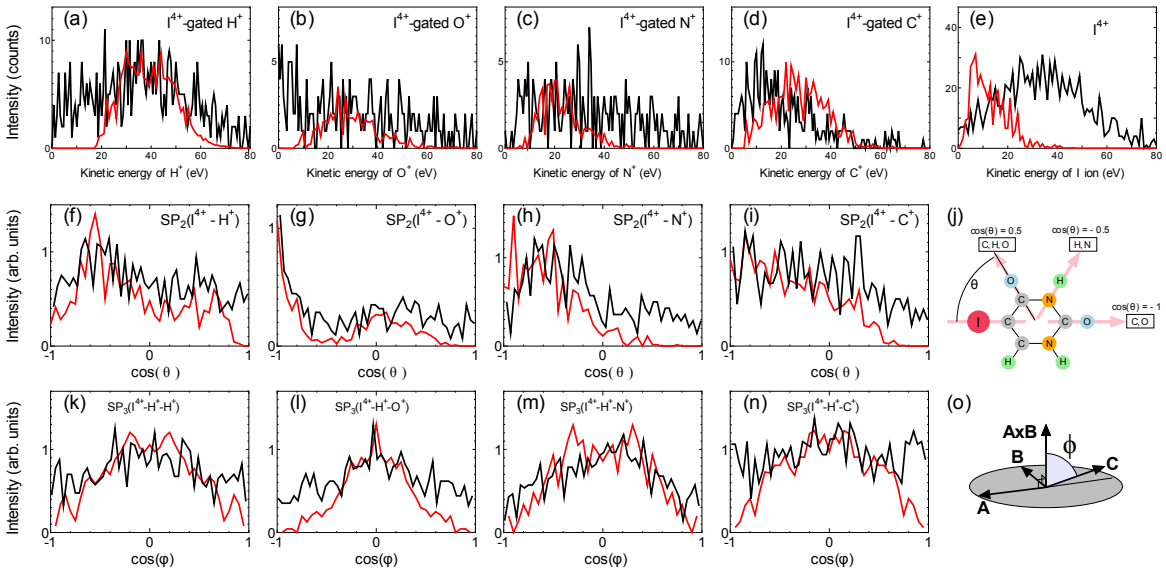

Fig. S4. Comparison between the experiment (black line) and CCE-CE model sumulations (red lines) for I^{4+} coincience data. (a)-(e) : Kinetic energy distribution of fragment ions. (f)-(i): $SP_2(I^{4+},X)$ for X=H^+, O^+, N^+ and C^+. (j): Schematics of molecular structure. (k)-(n): $SP_3(I^{4+},H^+, X)$ for X=H^+, O^+, N^+ and C^+. (o) Definition of ϕ.

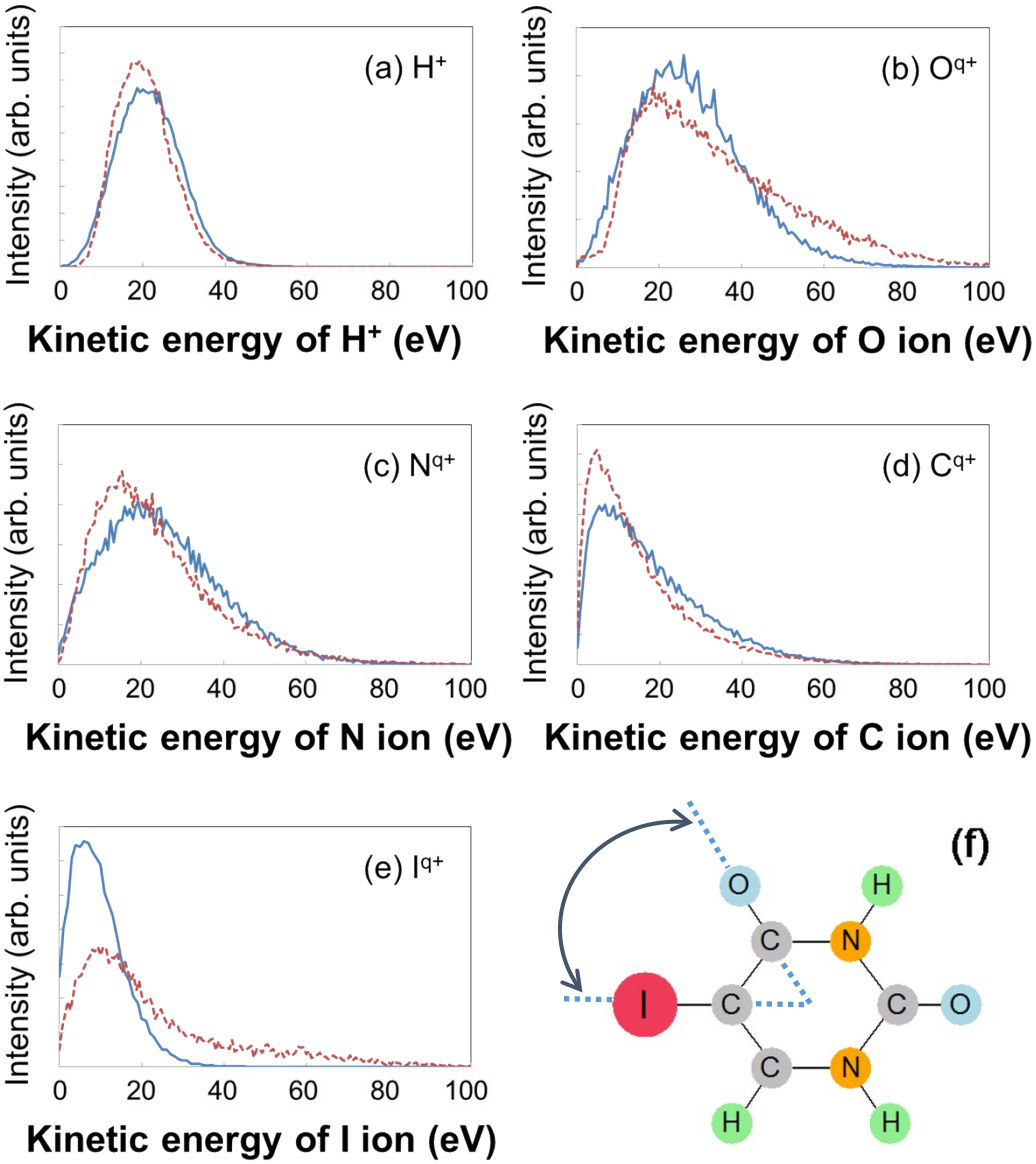

Fig. S5 SCC-DFTB results for the kinetic energy distribution (KED) of fragment ions emitted from 5-iodouracil: (a) H^+, (b) O^{q+}, (c) N^{q+}, (d) C^{q+} and (e) I^{q+}. The blue solid and red broken lines denote the SCC-DFTB results for $\Delta \vec{p}_{i\perp} = 0$ and $\Delta \vec{p}_{i\perp} \neq 0$, respectively. The other parameters used are the same as in the SCC-DFTB results of Figs. 5 and 6: $T = 300$ K, $\tau = 10$ fs, $\varepsilon = 6$ eV and $T_e = 6$ eV. (f) The definition of the equilibrium angle between two atoms (the I atom and its nearest O atom) in the neutral 5-IU molecule.

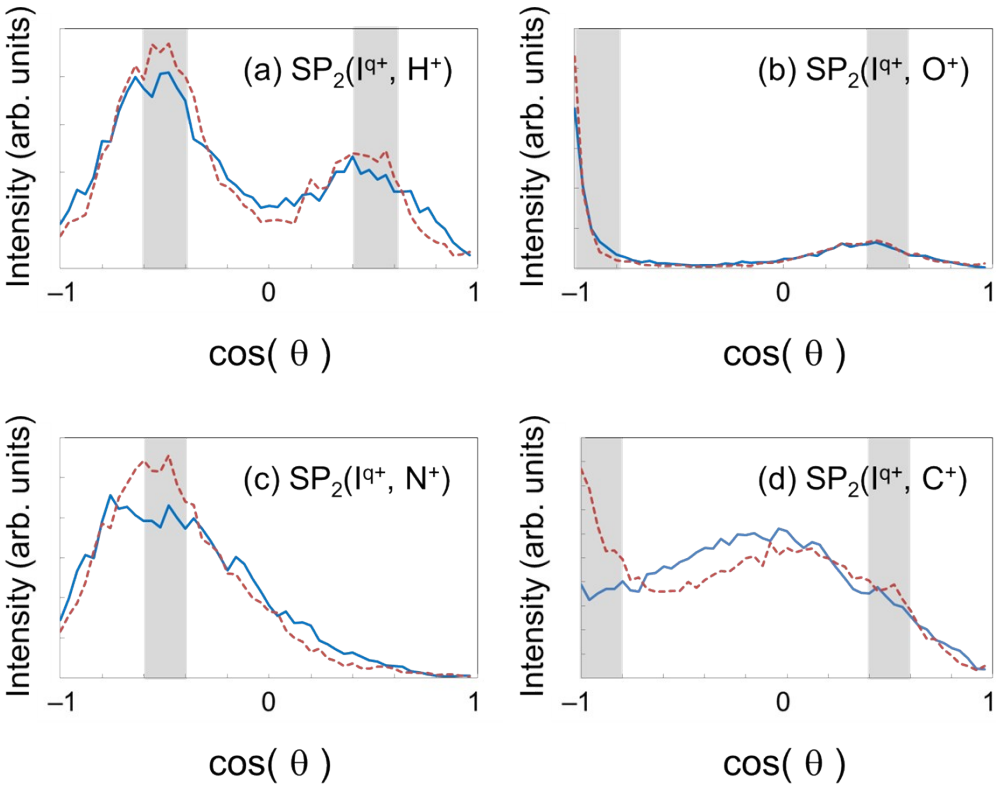

Fig. S6. Distribution of the normalized scalar product of momentum vectors, $SP_2(A,B)$, as a function of $\cos(\theta) = \vec{P}_A \cdot \vec{P}_B / |\vec{P}_A||\vec{P}_B|$ for fragment ion pairs (a) I^{q+}-H^+, (b) I^{q+}-O^+, (c) I^{q+}-N^+, and (d) I^{q+}-C^+. Gray shaded areas indicate the equilibrium angles between two atoms A and B as defined in Fig. S5 (f) . The blue and red broken lines denote the SCC-DFTB results for $\Delta \vec{p}_{i\perp} = 0$ and $\Delta \vec{p}_{i\perp} \neq 0$, respectively. The other parameters used for the SCC-DFTB simulation are the same as in Fig.S5: $T = 300$ K, $\tau = 10$ fs, $\varepsilon = 6$ eV and $T_e = 6$ eV.

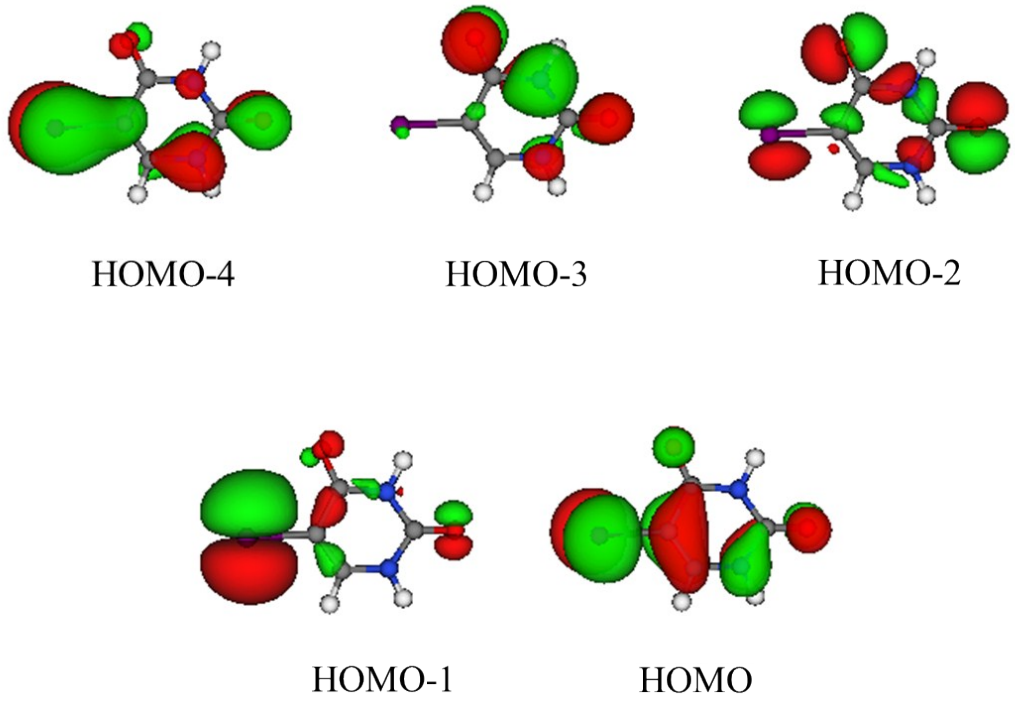

Fig. S7. Spatial distribution of electronic wave functions at t=0 fs, for HOMO, HOMO-n (n=1-4) of 5-IU, where the isosurfaces at the values of -0.03 e/a_0^3 and 0.03 e/a_0^3 are represented by red and green colors, respectively.